Uridine, a Sustainable Insulin Secretagogue, Inhibits UDP-Glucose and Cereblon Dependent Proinsulin Degradation

Takeshi Imai (timai@ncgg.go.jp)
National Center for Geriatrics and Gerontology
Jaeyong Cho
National Center for Geriatrics and Gerontology
Yoji Tsugawa
National Center for Geriatrics and Gerontology
Atsushi Miyajima
Nagoya Institute of Technology
Kazuki Yamaguchi
Nagoya Institute of Technology
Wakana Abe
Nagoya Institute of Technology
Hatsuo Yamamura
Nagoya Institute of Technology

Research Article

Keywords:

Posted Date: February 15th, 2022

DOI: https://doi.org/10.21203/rs.3.rs-1316195/v1

Abstract

Insulin secretion is regulated in multiple steps, and one of the main steps is in the endoplasmic reticulum (ER). Here, we show that UDP-glucose induces proinsulin ubiquitination by cereblon (CRBN), and uridine binds and competes for proinsulin degradation and behaves as sustainable insulin secretagogue. Using insulin mutagenesis of neonatal diabetes variant-C43G and maturity-onset diabetes of the young 10 (MODY10) variant-R46Q, UDP-glucose:glycoprotein glucosyltransferase 1 (UGGT1) protects CRBN-dependent proinsulin ubiquitination in the ER. CRBN is a ligand-inducible E3 ubiquitin ligase, and we found that UDP-glucose is the first identified endogenous proinsulin protein degrader. Uridine-containing compounds, such as uridine, UMP, UTP, and UDP-galactose, inhibit CRBN-dependent proinsulin degradation and stimulate insulin secretion from 3 to 24 h after administration in β-cell lines as well as mice. This late and long-term insulin secretion stimulation is designated a day sustainable insulin secretion stimulation. Uridine-containing compounds are designated sustainable insulin secretagogues.

1 Introduction

Insulin secreted from pancreatic β cells plays a central role in glucose homeostasis, and the impairment in insulin secretion leads to diabetes [1–4]. Hypoinsulinemia in insulin variants is found in maturity-onset diabetes of the young (MODY) 10 and neonatal diabetes. MODY is a form of diabetes caused by mutations in an autosomal dominant gene. Specifically, MODY10 [6–13] harbors insulin variants. Mechanistically, insulin variants in MODY10 are considered to cause diabetes due to impaired processing of insulin leading to hypoinsulinemia proinsulinR46Q variant [13] or impaired insulin receptor signaling in case of R89H-variant [14]. More severe hypoinsulinemia of the insulin variant of C43G [15] is neonatal diabetes. The difference in MODY10 and neonatal diabetes is not yet known. Here, we found two different reasons for genetic hypoinsulinemia. One is that proinsulinR46Q is retained in the endoplasmic reticulum (ER) and not secreted. The other is that proinsulinC43G is ubiquitinated and degraded and then not secreted.

Insulin is secreted by stress response. One of the unfolding protein responses (UPRs) is ER-associated protein degradation (ERAD). Under (oxidative) stress, unfolding protein is eliminated by HMG-CoA reductase degradation 1 (HRD1) in the ER. Another candidate ubiquitin ligase in the ER is CRBN [16]. Here, we found that even the proinsulinWT protein was also degraded by the ERAD system, indicating that inhibiting proinsulin degradation leads to insulin secretion stimulation.

Insulin secretagogues, such as glucose and arginine, stimulate insulin secretion immediately and are soon reduced [17, 18]. It forms one sharp peak [17, 18]. Here, using inhibition of the proinsulin ERAD system, we found several chemicals that induce daily sustainable insulin secretion.

2 Results

2.1 The R46 residue of proinsulin is involved in arginine-induced insulin secretion (Figure 1 and S1).

We previously reported that proinsulin increases its binding to UGGT1 and is retained in the endoplasmic reticulum (ER) when β-cell lines and mouse pancreases are maintained under arginine-depleted conditions [17]. Arginine administration releases proinsulin from UGGT1 in the ER and causes new complex formation between arginine and UGGT1. To assess the physiological importance of this interaction, we performed mutagenesis of the proinsulin gene to express the proinsulin variant associated with MODY 10 (maturity-onset diabetes of the young). Among four arginine residues (R46, R55, R56 and R89) in proinsulin, three variants (R46Q, R55C, R89H) are reported to cause MODY10 [4–9, 13, 14, 27–29]. R55, R56 and R89 are cleavage sites of protein convertase (PC1 and 2) [4, 13, 14, 19–21], and R46 is only one arginine residue of a noncleavage site. Therefore, we chose two MODY 10 variants of proinsulin, R46Q and R89H, and tested the impact of the mutations on glucose- or arginine-induced secretion in NIT1 cells (Fig. 1a). Both arginine and glucose strongly induced WT insulin secretion, as expected. Glucose failed to induce secretion of MODY10 variants of R46Q and R89H insulin (Fig. 1a). Interestingly, arginine administration significantly induced R89H-insulin secretion but not R46Q-insulin secretion (Fig. 1a), indicating that the R46 residue is involved in arginine-induced insulin secretion.

The PDB database (DOI: 10.2210/pdb3w7y/pdb) of proinsulin predicts that R46 is surrounded by a ring structure formed by valine 42 (V42), cysteine 43 (C43), glutamate 45 (E45), E106, C109, and asparagine 110 (N110) and protrudes from the plane formed by the ring (Fig. 1b and S1a). When a change in the three-dimensional structure of R46Q proinsulin was predicted using PyMOL software, the R46Q residue did not protrude from the ring (Fig. 1b and S1a). Immunoprecipitation of UGGT1 showed that the WT but not the R46 proinsulin residue interacts with UGGT1 in an arginine-dependent manner (Fig. 1c-e, S1b-S1d). We tested three insulin variants of C43G-neonatal diabetes, E45R and C109R, involving amino acids forming the ring structure, V42, C43, E45, E106, C109(-C43) and N110. C43G and C109R are associated with neonatal diabetes [14, 20, 21]. In agreement with immunoprecipitation of UGGT1, immunoprecipitation of WT insulin showed coprecipitation of UGGT1 that was lost in the presence of arginine. R46Q insulin maintains interaction with UGGT1 even in the presence of arginine. In contrast, three mutants involving the ring structure failed to interact with UGGT1 even in the absence of arginine, indicating that these residues are critical for the interaction of proinsulin with UGGT1 in the absence of arginine at the ER (Fig. 1e and S1e). Collectively, proinsulinWT is bound to UGGT1 in the absence of arginine and released from UGGT1 upon arginine administration, promoting secretion. In contrast, a MODY 10 variant of proinsulinR46Q is capable of binding to UGGT1 under arginine depletion but is unable to be released by arginine, preventing arginine-induced secretion of R46Q-insulin secretion.

2.2 Impaired UGGT1-interaction in the C43G-neonatal diabetes variant (Figure 2 and S2).

Next, we performed further characterization of three mutants of acidic amino acids that form ring structures around the R46 residue, C43G, E45R and C109R (Fig. 1b, 1e, S1a, and S1d). When

proinsulinWT showed binding to UGGT1 only in the absence of arginine, none of three mutants (C43G, E45R, or C109R) showed binding to UGGT1 either in the presence or absence of arginine, indicating that they may not be retained at the ER where UGGT1 resides (Fig. 2a).

We previously reported that arginine prevents the degradation of glucokinase by the E3 ubiquitin ligase cereblon (CRBN) using CRBN KO cells [22]. Thus, we tested whether degradation of proinsulinC43G is increased and mediated by CRBN. Indeed, proinsulinC43G showed ubiquitination only in NIT cells expressing CRBN (Fig. 2d, S2a). We previously reported that CRBN interacts with damage-specific DNA binding protein 1 (DDB1, [22]) for ubiquitination because they are two components of cullin ring ubiquitin ligase 4 (CRL4). In agreement with the interaction of proinsulinC43G with CRBN, proinsulinC43G interacted with DDB1 in CRBN+ cells but not in CRBN-KO cells (Fig. 2d and S2c) in the presence or absence of arginine. Then, we analyzed whether CRBN contributes to arginine-induced C43G-insulin secretion (Fig. 2b-d, S2a, b). The secretion of C43G mutant insulin in response to arginine was blunted compared with WT insulin in NIT1 cells expressing CRBN (Fig. 2b, c). The impairment in arginine-induced insulin secretion was not rescued by CRBN knockout in NIT1 cells expressing the C43G variant (Fig. 2c and S2b).

Collectively, these data indicated that proinsulinC43G interacts with CRBN and DDB1 instead of UGGT1, which leads to ubiquitination of proinsulinC43G by CRBN and subsequent degradation (Fig. 2e). Both proinsulinWT and proinsulinR46Q interact with UGGT1 in the absence of arginine (Fig. 2e). Whereas proinsulinWT is released from UGGT1 and secreted when arginine becomes available, the R46Q variant does not compete with arginine and remains bound to UGGT1, leading to ER retention and reduced secretion (Fig. 2e).

Based on two mutants, we propose that R46 and C43 of proinsulin have a distinct role in mediating arginine-induced insulin secretion. The R46 residue competes with arginine for the interaction with UGGT1, and the C43 residue mediates binding regardless of the availability of arginine. Thus, two variants (R46Q and C43G) responsible for MODY and neonatal diabetes cause impaired arginine-induced insulin secretion due to altered interaction with UGGT1.

2.3 Arginine switches proinsulin associated E3 ubiquitin ligases from HRD1 to CRBN (Figure 3 and S3).

In Fig. 2, we demonstrate that UGGT1 not only retains proinsulin in the ER but also protects proinsulin from ubiquitination and degradation by CRBN. This protection is releasing by arginine-replacing. Ubiquitination occurs on the lysine residue of K88-proinsulin. Nonubiquitinated K88R-proinsulin actually existed at much higher levels than WT-proinsulin (Fig. 3a). This indicates that WT proinsulin in the ER is ubiquitinated and degraded. Nonubiquitinated proinsulin K88R was secreted much more highly than WT proinsulin (Fig. S3a).

Proinsulin is one of the forms of insulin in the ER and the Golgi body [1, 2], leading to proinsulin ubiquitination called ERAD (ER-associated degradation). The main E3 ubiquitin ligase in ERAD is thought

to be HRD1 (HMG-CoA reductase degradation protein 1) [23–25]. Other E3 ubiquitin ligases, CRL4 (CUL4-DDB1-CRBN), also include proinsulin ubiquitination (Fig. 2). First, arginine-induced proinsulin ubiquitination enzymes were investigated (Fig. 3b and 3c). Arginine administration induces proinsulin-associated DDB1 (Fig. 3b); nevertheless, arginine administration reduces proinsulin-associated HRD1 (Fig. 3c). On the other hand, UGGT1-associated E3 ubiquitin ligases were also analyzed. UGGT1 was also associated with DDB1 after arginine administration (Fig. 3d), but HRD1 dissociated after arginine administration (Fig. 3e). In fact, proinsulin and UGGT1 were mainly degraded after arginine administration (Fig. 3a and 3f), indicating that CRL4 (CUL4-DDB1-CRBN) is the E3 ubiquitin ligase that ubiquitinates and degrades proinsulin and UGGT1 after arginine administration. CRBN colocalizes with UGGT1 in the ER with UDP-glucose and arginine (Fig. S3b).

2.4 Uridine and succinimide protect proinsulin degradation from CRBN and stimulate insulin secretion from 3 h to 24 h (Figure 4 and S4).

Therefore, we demonstrate that UGGT1 protects against proinsulin ubiquitination by CRL4 (CUL4-DDB1-CRBN), and arginine administration releases this protective effect (Fig. 3), indicating that arginine-induced insulin secretion is a new step in inducing proinsulin degradation. If, this degradation is reduced, stimulating insulin secretion as a drug target such as K88R-insulin (Fig. 3a and S3a).

How repress CRBN-dependent ubiquitination? CRBN is ligand-induced ubiquitination. First identified exogenous ligand is thalidomide [22]. Its substrate (ubiquitinated) protein is Ikaros [26]. A possible endogenous ligand is uridine [27], but its substrate protein is not known. MEIS2 has been identified as an unknown endogenous/natural ligand A by competing with thalidomide [26]. Another exogenous ligand is succinimide [27]. CRBN-binding chemicals, such as uridine and succinimides, bind to CRBN and compete for endogenous/natural ligand A or proinsulin degrader X (Fig. S4c).

First, we administered uridine to NIT1 cells (Fig. 4a-c) and C57BL/6J mice (Fig. 4d and 4e). Uridine released proinsulin degradation by endogenous proinsulin degrader X and increased proinsulin protein levels (Fig. 4a). Uridine administration induced insulin secretion in a dose-dependent manner (Fig. 4b). Surprisingly, uridine-induced insulin secretion occurs from 3 to 24 h (Fig. 4b) because general insulin secretions, such as glucose and arginine, induce insulin secretion in minutes [17, 18]. This induction was not observed in CRBN KO cells (Fig. 4c), indicating that uridine-competitive proinsulin degradation occurs through CRBN. Uridine administration to C57BL6 mice also induced insulin and reduced glucose concentrations from 3 to 24 h (Fig. 4d and 4e). Taken together, uridine-induced insulin secretion starts late and sustainably. Note that other uridine-containing chemicals, UMP and UTP, also induced insulin secretion (Fig. 4f) sustainably.

Succinimide (Fig. 4g and 4h) is an artificial CRBN-binding chemical [27] and is a smaller molecule than uridine. Succinimide might not have a substrate protein-binding motif and has a higher affinity for CRBN than uridine [27], indicating that succinimide may behave as a stronger CRBN inhibitor and stimulate insulin secretion than uridine. In fact, succinimide binds to CRBN, protects proinsulin degradation from proinsulin degrader X in a dose-dependent manner (Fig. 4g), and sustainably stimulates insulin secretion

(Fig. 4h). Succinimide stimulates insulin secretion more than uridine does (Fig. 4i). The IC_{50} of succinimide was 1.541 μM (Fig. S4a), and the IC_{50} of uridine was 0.3473 μM (Fig. S4b).

2.5 UDP-glucose is an endogenous proinsulin protein degrader through CRBN.

UDP-glucose and succinimide glucose degrade insulin (Figure 5 and S5).

We explored uridine monosaccharide to identify the proinsulin protein degrader X. Similar to uridine (Fig. 4), UDP-galactose also stimulated insulin secretion in β cells (Fig. 5a), while UDP-glucose repressed insulin secretion (Fig. 5a). These data indicated that UDP-glucose is the proinsulin degrader X. Uridine binds to CRBN (Fig. 4), and glucose weakly binds to proinsulin (Fig. 5b). Nevertheless, galactose does not bind to proinsulin (Fig. 5b). These data suggested that UDP-glucose combined with CRBN and proinsulin. UDP-glucose administration to NIT1 cells reduced proinsulin in a dose-dependent manner (Fig. 5c, S5b-d, IC50=1.322 μM). UDP-glucose administration to C57/BL6J mice reduced insulin concentrations (Fig. 5d) and induced glucose concentrations (Fig. 5e) from 3 h to 24 h.

Succinimide binds to CRBN with higher affinity than uridine (Fig. 4, and [27]), indicating that succinimide-linker-glucose may behave as a proinsulin degrader. We synthesized two linker lengths (C_2H_4 and C_6H_{12}), and the linkers were combined with succinimide and glucose. Succinimide-C2-glucose (C2) and succinimide-C6-glucose (C6) were synthesized and analyzed. In vitro complex formation analysis showed that UDP-glucose and C6 stimulated complex formation weakly, and C2 stimulated complex formation strongly (Fig. 5f). UDP-glucose and C6 degraded proinsulin in a dose-dependent manner (Fig. 5c), although surprisingly, C2 induced proinsulin protein in a dose-dependent manner (Fig. 5g). These phenomena are reproducible for insulin secretion (Fig. 5h). UDP-glucose and C6 reduce insulin secretion, and C6 induces insulin secretion in a dose-dependent manner. Note: UDP-glucose-IC_{50} = 1.322 μM (Fig. S5b-d), C2-IC_{50} = 0.475 μM (Fig. S5e-g), C6-IC_{50} = 0.489 μM (Fig. S5h-j).

3 Conclusion

We previously reported that proinsulin is retained in the ER through binding to the ER resident protein UGGT1 when the availability of arginine is low and that arginine releases proinsulin from the ER through competition with UGGT1 [17]. Here, we report MODY10- or neonatal diabetes-associated proinsulin variants that interfere with their interaction with UGGT1. Through the analysis of these variants, we further refined the molecular basis of the interaction between proinsulin and UGGT1. Proinsulin binds to UGGT1 via the R46 residue and amino acid residues that form a ring around R46 when the availability of arginine is low in the ER, causing the retention of proinsulin in the ER of pancreatic β cells. The C43, E45, and C109 residues of proinsulin form a ring structure that mediates the binding of proinsulin to UGGT1. In support of this hypothesis, C43G and C109R variants of proinsulin associated with neonatal diabetes failed to bind UGGT1. These variants bind the CRL4 E3 ubiquitin ligase of CRBN and DDB1 instead, leading to degradation after ubiquitination both in the presence and absence of arginine. When the

availability of arginine increases in the ER of pancreatic β cells, arginine disrupts binding between proinsulin and the C-terminal domain of UGGT1 competitively, resulting in the release of proinsulin from UGGT1. This allows proinsulin to be further processed at the Golgi network and mature into secretory vesicles for insulin secretion. ProinsulinR46Q and proinsulinC43G genetic mutations associated with MODY/neonatal diabetes all cause impairment in arginine-inducing insulin secretion but cause distinct defects in the interaction between UGGT1 and proinsulin.

Free proinsulinWT also interacts with UDP-glucose and CRBN+DDB1 after dissociation from UGGT1 and is ubiquitinated. UDP-glucose and proinsulin are the first identified endogenous CRBN ligands and their substrate proteins.

This UDP-glucose-dependent proinsulin degradation is associated with linker length and is important. A shorter linker (C2) strengthens the complex, and proinsulin is degraded. A longer linker (C6) makes the complex weaker, but proinsulin is not ubiquitinated.

Using uridine or succinimide, proinsulin degradation by UDP-glucose and CRBN was inhibited, and insulin secretion was induced from 3 to 24 h (Fig. 4). Generally, insulin secretion stimulation is in minutes [17, 18]. Insulin secretagoues (glucose, arginine, etc.) activate glucokinase activity and UGGT1 ER retention and stimulate insulin secretion immediately. Instead of acute induction by insulin secretagogues, uridine, succinimide and succinimide-C6-glucose stimulation starts late and sustainably. They might be developing a new anti-diabetes drug.

4 Discussion

4-1. Proinsulin ERAD by CRBN controlled by uridine and UDP-glucose.

ER-associated protein degradation (ERAD) is one unfolded protein response (UPR) cascade that eliminates unfolded proteins. Generally, unfolded proteins in the ER are ubiquitinated by HRD1. The HRD1 ubiquitination system is controlled by oxidative stress. Here, we identify other E3 ubiquitin ligase CRBN. CRBN is ligand-inducible E3 ubiquitin ligase. The first identified ligand is thalidomide, and the thalidomide-CRBN substrate protein is Ikaros [26]. In addition, we identified two types of CRBN ubiquitination signaling molecules: agonists (UDP-glucose) and antagonists (uridine). Both are endogenous chemicals that always exist in each cell. This indicates endogenous chemical control of the ERAD system. As described above, the existence of unfolding proteins triggers ERAD but does not control other molecules. This is the first evidence of endogenous chemicals controlling ERAD and UPR.

4-2. Uridine-induced and UDP-glucose-reduced sustainable insulin secretion

Not only unfolded proinsulinC43G mutated protein but also proinsulinWT protein were degraded by CRBN (Fig. 3 and 4). An agonist of proinsulin degradation is UDP-glucose, and a CRBN-binding antagonist is uridine. Both agonists and antagonists have effects from 3 to 24 h. This long-term (approximately 1 d) induction and reduction is exceptional for insulin secretion.

5 Methods

5.1 Antibodies and cell culture

The following antibodies were purchased: β-actin (sc-47778, Santa Cruz Biotechnology, Santa Cruz, CA, USA), glyceraldehyde 3-phosphate dehydrogenase (ab9485, Abcam, Cambridge, UK), insulin (L6B10, Cell Signaling Technology, Danvers, MA, USA, and sc-9168, Santa Cruz Biotechnology), UGGT1 (14170-1-AP, Proteintech, Rosemont, IL, USA; sc-374565, Santa Cruz Biotechnology; and ab13520-50, Abcam), FLAG (F-1804, Sigma, St. Louis, MO, USA), and Alexa Fluor-conjugated secondary antibodies (Thermo Fisher, Rockford, IL, USA). Mouse pancreas-derived NIT-1 cells (CRL-2055TM purchased from ATCC, Manassas, VA, USA) were maintained as described previously [17, 18, 28–32]. Briefly, the cells were plated at a density of 1.5–3.0 × 106 cells/60-mm dish with replacement of F-12K medium (Kaighn's modification of Ham's F-12 medium containing 2.419 mM L-arginine) plus 10% fetal calf serum (FCS) after 48 h of culture. Human embryo kidney 293T (HEK293T) cells and human hepatocellular carcinoma (HepG2) cells were maintained with DMEM+10% FCS [23, 24, 28–32].

5.2 Analysis of insulin secretion from cells.

Insulin secretion was determined using a commercial enzyme-linked immunosorbent assay (ELISA) kit (Shibayagi, Gunma, Japan) [17, 18] as described previously. Briefly, the culture medium of the NIT-1 cells was replaced with L-arginine-free F12K (7 mM glucose) +10% fetal calf serum (FCS) for 30 min, followed by L-arginine administration (1 mM) for 5 min. Subsequently, the medium was collected for insulin measurement. We did not use phosphate-buffered saline (PBS) or Krebs–Ringer HEPES buffer because slight cell damage was detected with PBS/KRH without FCS even in 30 min. Insulin concentration was measured using an ELISA kit (Shibayagi, Gunma, Japan). Secretion of mutated insulin (i.e., R46Q-INS variant) secretion was analyzed using an anti-Myc antibody. Secreted myc was measured with an ELISA kit (ab277452, Abcam).

5.3 Immunoprecipitation and Western blot

Immunoprecipitation and Western blot analysis were performed as described previously with minor modifications [17, 18, 28–32]. NIT-1 cells transfected with the pCDNA-insulin-Myc expression vector were cultivated in arginine-free medium for 30 min before arginine was added. Cells were lysed in buffer containing 20 mM HEPES-NaOH (pH 7.9), 1 mM MgCl2, 0.2 mM CaCl2, 100 mM KCl, 0.2 mM EDTA, 10% glycerol, 0.1% Nonidet P-40, 1 mM dithiothreitol, 0.2 mM phenylmethylsulfonyl fluoride (Nacalai Tesque, Kyoto, Japan), and 3% n-octyl-β-D-glucoside (DOJINDO, Tokyo, Japan). After incubation on ice for 30 min, lysates were centrifuged at 12,000 g for 15 min at 4°C and dialyzed for 3 h at 4°C to lysis buffer without n-octyl-β-D-glucoside. After dialysis, the supernatant was incubated with the indicated antibody for 120 min at 4°C. The samples were then incubated with Protein G Sepharose 4 Fast Flow (GE Healthcare). After an additional washing, the precipitates were heat-denatured in SDS-sample buffer. For immunoblot analysis, proteins were separated by SDS/PAGE and transferred to a PVDF membrane for Western blot analysis. The membranes were blocked with 5% nonfat milk and Tris-buffered saline with Tween 0.1%,

incubated overnight with a mixture of primary antibody (c-Myc [1:1000]) and Can Get Signal solution (TOYOBO, Osaka, Japan) at 4°C, washed, incubated with the secondary antibody for 60 min at room temperature, and then washed again. Immune complexes were detected using Immunostar LD (Wako) substrate. Signals were quantified with the LAS 4000 imaging system (GE Healthcare). ImageJ was used for densitometry of scanned membranes.

5.4 Structure analysis

Homology models of human proinsulin were generated using the Swiss-Model server. The template with the highest quality (2kqp.1; PDB ID: 2KQP) [33] was selected for model building. Computer modeling of R46Q was performed using the PyMOL mutagenesis algorithm wherein the backbone-dependent rotamers of glutamine were examined. Only the rotamer with the highest frequency of appearance in proteins is shown. Global and per-residue model quality was evaluated using the QMEAN4 scoring function. The obtained scores were −5.83 and −6.06 for wild-type and mutant humans, respectively.

5.5 Proinsulin mutants

Using mutated synthesized oligomers and a PrimeSTAR mutagenesis basal kit (Takara, Kyoto, Japan), mutated insulin and UGGT1 expression vectors were produced. NIT-1 cells were transfected with pCDNA-insulin (WT, C43G, E45R, R46Q or C109R)-Myc expression vectors with Lipofectamine 2000 (Thermo Fisher, Rockford, IL, USA). On the next day, these cells were cultivated in arginine-free medium for 30 min before arginine was added. The supernatants were analyzed with a Myc-ELISA kit (Shibayagi, Japan). The transfection efficiency was ~10% for NIT-1 cells and 80% for HEK293FT cells.

5.6 Chemical synthesis

General

1H and 13C NMR spectra were recorded in CDCl3-d and D2O using a Bruker AVANCE 400 Plus Nanobay instrument (400 and 101 MHz) and a Bruker AVANCE 500 instrument fitted with a cryoprobe (500 and 126 MHz), respectively. Chemical shifts (δ) are given in ppm and referenced to tetramethylsilane (0.00 ppm) or the internal solvent signal used as an internal standard. Assignments in the NMR spectra were made by first-order analysis of the spectra and were supported by 1H−1H COSY and 1H−13C HMQC correlation results. Matrix-assisted laser desorption ionization time-of-flight high-resolution mass spectrometry (MALDI-TOF HRMS) spectra were recorded on a Jeol JMS-S3000 using 2,5-dihydroxylbenzoic acid as the matrix. Unless otherwise stated, all commercially available solvents and reagents were purchased from FUJIFILM Wako Pure Chemical Corporation and Tokyo Chemical Industry Company Limited without further purification.

2-Bromoethyl 2,3,4,6-tetra-O-acetyl-β-D-glucopyranoside (2)

To a solution of compound 1 (3.00 g, 6.09 mmol) and 2-bromoethanol (743 µL, 10.4 mmol) in dichloromethane (28.4 mL) was added molecular seives 3Å powder (3.00 g), and cooled at −40°C. To the mixture was added boron trifluoride-ethyl ether complex (229 µL, 1.82 mmol) diluted in dichloromethane

(2.1 mL) and stirred at −40°C for 30 min. The solution was diluted with dichloromethane and filtered through celite. The filtrate was washed with aqueous sodium hydrogen carbonate and brine, dried over anhydrous sodium sulfate, filtered, and evaporated. The residue was purified by silica gel chromatography with 8:1 to 4:1 (v/v) hexane-ethyl acetate to give 2 (1.84 g, 66%): 1H NMR (CDCl3, 400 MHz) δ 5.22 (t, 1 H, J2,3 =9.5 Hz, H-3), 5.09 (t, 1 H, J3,4 =9.5 Hz, H-4), 5.02 (dd, 1 H, Hz, H-2), 4.58 (d, 1 H, J1,2 = 8.0 Hz, H-1), 4.58 (dd, 1 H, J = 4.8 Hz,, J6a,6b = 12.3 Hz, H-6a), 4.20-4.13 (m, 2 H, H-6b, -OCH2-), 3.85-3.79 (m, 1 H, -OCH2-), 3.74-3.69(m, 1 H, H-5), 3.49-3.45 (m, 2 H, -CH2Br), 2.10 (s, 3 H, Ac), 2.08 (s, 3 H, Ac), 2.03 (s, 3 H, Ac), 2.02 (s, 3 H, Ac); 13C{1H} NMR δ (CDCl3, 101 MHz): 170.6, 170.2, 169.4, 169.4, 101.0, 72.6, 71.9, 71.0, 69.8, 68.3, 61.8, 29.8, 20.7, 20.6, 20.5.

6-Bromohexyl 2,3,4,6-tetra-O-acetyl-β-D-glucopyranoside (3)

To a solution of compound 1 (3.00 g, 6.09 mmol) and 6-bromoethanol (2.49 mL, 10.3 mmol) in dichloromethane (28.4 mL) was added molecular sieves 4 Å powder (3.00 g) and cooled at −40°C. To the mixture was added boron trifluoride-ethyl ether complex (229 µL, 1.82 mmol) diluted in dichloromethane (2.1 mL) and stirred at −40°C for 30 min, at −20°C for 30 min and then at 0°C for 30 min. The solution was diluted with dichloromethane and filtered through celite. The filtrate was washed with aqueous sodium hydrogen carbonate and brine, dried over anhydrous sodium sulfate, filtered, and evaporated. The residue was purified by silica gel chromatography with 10:1 to 3:1 (v/v) hexane-ethyl acetate to give 3 (2.06 g, 66%): 1H NMR (CDCl3, 400 MHz) δ 5.21 (t, 1 H, J2,3 =9.5 Hz, H-3), 5.09 (t, 1 H, J3,4 =9.7 Hz, H-4), 4.99 (dd, 1 H, Hz, H-2), 4.49 (d, 1 H, J1,2 = 8.0 Hz, H-1), 4.27 (dd, 1 H, J = 4.7 Hz,, J6a,6b = 12.3 Hz, H-6a), 4.14 (dd, 1 H, J5,6a = 2.4 Hz, H-6b), 3.91-3.85 (m, 1 H, -OCH2-), 3.72-3.67 (m, 1 H, H-5), 3.51-3.46 (m, 1 H, -OCH2-), 3.41 (t, 2 H, J = 6.8 Hz, -CH2Br), 2.11 (s, 3 H, Ac), 2.05 (s, 3 H, Ac), 2.03 (s, 3 H, Ac), 2.01 (s, 3 H, Ac), 1.89-1.82 (m, 2 H, -CH2-), 1.62-1.55 (m, 2 H, -CH2-), 1.46-1.32 (m, 4 H, -CH2-); 13C{1H} NMR (CDCl3,101 MHz) δ 170.7, 170.3, 169.4, 169.2, 100.8, 72.8, 71.7, 71.3, 69.9, 68.4, 62.0, 33.7, 32.6, 29.2, 27.7, 25.0, 20.7, 20.6, 20.6, 20.6.

2-S-Thioacetylethyl 2,3,4,6-tetra-O-acetyl-β-D-glucopyranoside (4)

To a solution of compound 2 (500 mg, 1.10 mmol) and thioacetic acid (117 µL, 1.64 mmol) in N,N-dimethylformamide (3.67 mL) was added potassium carbonate (228 mg, 1.65 mmol) and stirred at room temperature for 12 h. The solution was diluted with ethyl acetate, washed with aqueous sodium hydrogen carbonate and brine, dried over anhydrous sodium sulfate, filtered, and evaporated. The residue was purified by silica gel chromatography with 4:1 (v/v) hexane-ethyl acetate to give 4 (492 mg, 99%): 1H NMR (CDCl3, 400 MHz) δ 5.21 (t, 1 H, J2,3 =9.5 Hz, H-3), 5.09 (t, 1 H, J3,4 =9.7 Hz, H-4), 4.99 (dd, 1 H, Hz, H-2), 4.53 (d, 1 H, J1,2 = 8.0 Hz, H-1), 4.26 (dd, 1 H, J = 4.8 Hz,, J6a,6b = 12.3 Hz, H-6a), 4.14 (dd, 1 H, J = 2.4 Hz,, J6a,6b = 12.3 Hz, H-6b), 4.01-3.95 (m, 1 H, -OCH2-), 3.73-3.68 (m, 1 H, H-5), 3.65-3.59 (m, 1 H, H-5, -OCH2-), 3.26-3.01 (m, 2 H, -CH2S), 2.34 (s, 3 H, SAc), 2.09 (s, 3 H, Ac), 2.08 (s, 3 H, Ac), 2.03 (s, 3 H, Ac), 2.01 (s, 3 H, Ac); 13C{1H} NMR (CDCl3, 101 MHz) δ 195.2, 170.6, 170.2, 169.4, 169.3, 100.8, 72.7, 71.9, 71.1, 68.6, 68.3, 61.8, 30.5, 28.8, 20.7, 20.7, 20.6, 20.5.

6-S-Thioacetylhexyl 2,3,4,6-tetra-O-acetyl-β-D-glucopyranoside (5)

To a solution of compound 3 (700 mg, 1.37 mmol) and thioacetic acid (146 μL, 1.79 mmol) in N,N-dimethylformamide (4.57 mL) was added potassium carbonate (284 mg, 2.05 mmol) and stirred at room temperature for 17.5 h. The solution was diluted with ethyl acetate, washed with water and brine, dried over anhydrous sodium sulfate, filtered, and evaporated. The residue was purified by silica gel chromatography with 8:1 to 4:1 (v/v) hexane-ethyl acetate to give 5 (561 mg, 83%): 1H NMR (CDCl3, 400 MHz) δ 5.20 (t, 1 H, J2,3 =9.5 Hz, H-3), 5.09 (t, 1 H, J3,4 =9.7 Hz, H-4), 4.98 (dd, 1 H, Hz, H-2), 4.49 (d, 1 H, J1,2 = 8.0 Hz, H-1), 4.27 (dd, 1 H, J = 4.7 Hz,, J6a,6b = 12.3 Hz, H-6a), 4.14 (dd, 1 H, J = 2.4 Hz,, J6a,6b = 12.3 Hz, H-6b), 3.90-3.84 (m, 1 H, -OCH2-), 3.71-3.67 (m, 1 H, H-5), 3.50-3.44 (m, 1 H, H-5, -OCH2-), 2.85 (t, 2 H, J = 7.3 Hz -CH2S), 2.33 (s, 3 H, SAc), 2.09 (s, 3 H, Ac), 2.04 (s, 3 H, Ac), 2.03 (s, 3 H, Ac), 2.01 (s, 3 H, Ac), 1.59-1.52 (m, 4 H, -CH2-), 1.37-1.32 (m, 4 H, -CH2-); 13C{1H} NMR (CDCl3, 101 MHz) δ 196.0, 170.7, 170.3, 169.4, 169.3, 100.8, 72.9, 71.8, 71.3, 69.0, 68.5, 62.0, 30.6, 29.4, 29.2, 29.0, 28.4, 25.3, 20.8, 20.7, 20.6, 20.6.

2-S-Ethyl-β-D-glucopyranose S-linked maleimide (6) [34]

A solution of 4 (50.0 mg, 111 μmol) in methanol (950 μL) was added to 28% NaOMe-MeOH (50 μL) and then stirred at room temperature for 1 h. Diaion™ SK1B was added to the solution for quenching and filtration and evaporation. The residue was dissolved in methanol (2.22 mL), Et3N (22 μL) and maleimide (53.9 mg, 555 μmol) were added, and the mixture was stirred at room temperature for 1 h. The solution was concentrated, and the residue was purified by silica gel chromatography with 50:1 to 5:1 (v/v) dichloromethane-methanol to give 6 (30.3 mg, 81%): 1H NMR (D2O, 400 MHz) δ 4.30 (d, 1 H, J1,2 =8.0 Hz, H-1), 3.98-3.90 (m, 2 H, -CH2SCH-, -OCH2-), 3.75-3.72 (m, 2 H, H-6, -OCH2-), 3.53 (dd, 1 H, J5,6a= 6.0 Hz,, J6a,6b= 12.1 Hz, H-6), 3.31-3.25 (m, 2 H, H-3, H-5), 3.21-3.07 (m, 3 H, H-2, H-4, -SCHCH2-), 2.90-2.86 (m, 1 H, -CH2S-), 2.80-2.75 (m, 1 H, -CH2S-), 2.63-2.58 (m, 1 H, -SCHCH2-); 13C{1H} NMR (CDCl3, 126 MHz) δ 180.9, 179.7, 102.3, 75.8, 75.5, 72.9, 69.4, 69.0, 60.6, 41.5, 41.4, 37.2, 30.3; MALDI-TOF HRMS m/z: [M+Na]+: Calcd for C12H19N1O8S1+Na+: 360.0724; Found: 360.0676.

6-S-Hexyl-β-D-glucopyranose S-linked maleimide (7) [34]

A solution of 5 (50.0 mg, 101 μmol) in methanol (950 μL) was added to 28% NaOMe-MeOH (50 μL) and then stirred at room temperature for 2.5 h. Diaion™ SK1B was added to the solution for quenching, filtration, and evaporation. The residue was dissolved in methanol (2.02 mL), Et3N (20 μL) and maleimide (49.0 mg, 505 μmol) were added, and the mixture was stirred at room temperature for 1 h. The solution was concentrated, and the residue was purified by reverse-phase C18 silica gel chromatography with 1:0 to 4:1 (v/v) H2O-CH3CN to give 6 (27.5 mg, 72%): 1H NMR (D2O, 500 MHz) δ 4.32 (d, 1 H, J1,2 =8.0 Hz, H-1), 3.98-3.93-3.90 (m, 1 H, -CH2SCH-), 3.82-3.78 (m, 2 H, H-6a, -OCH2-), 3.61-3.52 (m, 2 H, H-6b, -OCH2-), 3.38-3.30 (m, 2 H, H-3, H-5), 3.27-3.10 (m, 3 H, H-2, H-4, -SCHCH2-), 2.67-2.57 (m, 3 H, -SCHCH2-, -CH2S-), 1.52-1.47 (m, 4 H, -CH2-), 1.32-1.24 (m, 4 H, -CH2-); 13C{1H} NMR (CDCl3, 126 MHz) δ 181.2, 179.9, 102.0, 75.8, 75.7, 73.0, 70.4, 69.5, 60.6, 41.4, 37.2, 30.0, 28.4, 28.1, 27.4, 24.4; MALDI-TOF HRMS m/z: [M+Na]+: Calcd for C16H27N1O8S1+Na+: 416.1350; Found: 415.1309.

5.7 Statistical analysis

The values are reported as the means ± standard error (n = 6). Statistical significance (single-sided Student's t test) is indicated in the figure legends as follows: *p < 0.05. n = 6 for statistical analysis [17, 18, 28–32]. For reproducibility of key experiments, we performed a total number of experiments exceeding ten times, including experiments for setting conditions with similar results. Additionally, we employed multiple approaches to confirm one result.

5.8 Ethical approval

The study is reported in accordance with ARRIVE guidelines. All mouse experiments were performed in accordance with the ethical guidelines for animal care of National Center for Geriatrics and Gerontology, and the experimental protocols were approved by the Animal Care Committee of National Center for Geriatrics and Gerontology [17,18, 28-32].

Abbreviations

RBN, cereblon

CRL4, cullin ring ubiquitin ligase 4

CUL4, cullin 4

DDB1, damage-specific DNA binding protein 1

ER, endoplasmic reticulum

ERAD, ER-associated protein degradation

ERRS, ER-retention signal

GCK, glucokinase

GLUT, glucose transporter

HOMAβ, homeostatic model assessment of β cells

HRD1, HMG-CoA reductase degradation 1

IC_{50}, half maximal (50%) inhibitory concentration

IP, immunoprecipitation

MODY, maturity-onset diabetes of the young

TCA cycle, tricarboxylic acid cycle

UGGT, UDP-glucose:glycoprotein glucosyltransferase

UPR, unfolded protein response

WB, Western blot

WT, wild type

Declarations

Acknowledgments

We are grateful to our department members at NCGG for their helpful discussions and Dr. N. Maekawa and M Umeda for technical assistance, Pr. T. Satoh at Nagoya City University for protein structure analysis, and Pr. T. Ito at Tokyo Medical University for CRBN KO cells.

Funding

This work was supported by a Grant-in-Aid from the Ministry of Education, Culture, Sports, Science and Technology (MEXT 18659493), the Japan Science and Technology Agency (A-STEP-AS2312036G and FY2013-SICP) and NCGG (28-25, 19-7, 21-3) to TI.

Author Contribution

JC, AM, KY, WA, YT, and HM performed the experiments, TI designed the experiments, analyzed the data, and wrote the manuscript.

Author Information

Readers are welcome to comment on the online version of the paper. Correspondence should be addressed to TI (timai@ncgg.go.jp).

Data and materials availability

Requests for data and materials should be addressed to TI (timai@ncgg.go.jp).

Competing interest

The authors declare no competing financial interests.

References

1. Rhodes CJ, Shoelson S, Halban PA, Insulin biosynthesis, processing, and chemistry, Joslin's Diabetes Mellitus Fourteenth Edition 2005 Chapter 5 pp65-pp82 (Lippincott Williams and Wilkins)

2. Herquin JC, Cell biology of insulin secretion, Joslin's Diabetes Mellitus Fourteenth Edition 2005 Chapter 6 pp83-pp108 (Lippincott Williams and Wilkins)
3. Chen, C., Cohrs, C.M., Stertmann, J., Bozsak, R. & Speier, S. Human beta cell mass and function in diabetes: Recent advances in knowledge and technologies to understand disease pathogenesis. Mol Metab **6**, 943–957 (2017).
4. Boland, B.B., Rhodes, C.J. & Grimsby, J.S. The dynamic plasticity of insulin production in beta-cells. Mol Metab **6**, 958–973 (2017).
5. Pueyo ME, Clement K, Vaxillaire M, Passa P, Froguel P, Robert JJ, Velho G. Arginine-Induced Insulin Release in Glucokinase-Deficient Subjects. Diabetes Care **17**, 1015–1021 (1994).
6. Støy J, E.L. Edghill, S.E. Flanagan, H. Ye, V.P. Paz, A. Pluzhnikov, J.E. Below, M.G. Hayes, N.J. Cox, G.M. Lipkind, R.B. Lipton, S.A. Greeley, A.M. Patch, S. Ellard, D.F. Steiner, A.T. Hattersley, L.H. Philipson, G.I. Bell. Neonatal Diabetes International Collaborative Group, Insulin gene mutations as a cause of permanent neonatal diabetes, Proc Natl Acad Sci USA **104**, 15040–15044 (2007)
7. Meur G, A. Simon, N. Harun, M. Virally, A. Dechaume, A. Bonnefond, S. Fetita, A.I. Tarasov, P.J. Guillausseau, T.W. Boesgaard, O. Pedersen, T. Hansen, M. Polak, J.F. Gautier, P. Froguel, G.A. Rutter, M. Vaxillaire M Insulin gene mutations resulting in early-onset diabetes: marked differences in clinical presentation, metabolic status, and pathogenic effect through endoplasmic reticulum retention, Diabetes **59**, 653–661 (2010).
8. Park SY, H. Ye, D. F. Steiner, G. I. Bell GI. Mutant proinsulin proteins associated with neonatal diabetes are retained in the endoplasmic reticulum and not efficiently secreted, Biochem Biophys Res Commun **391**, 1449–1454 (2010).
9. Rajan S, S.C. Eames, S.Y. Park, C. Labno, G.I. Bell, V.E. Prince, L.H. Philipson. *In vitro* processing and secretion of mutant insulin proteins that cause permanent neonatal diabetes, *Am J Physiol Endocrinol Metab* **298**, E403-E410 (2010).
10. Liu M, R. Lara-Lemus, S.O. Shan, J. Wright, L. Haataja, F. Barbetti, H. Guo, D. Larkin, P. Arvan. Impaired cleavage of preproinsulin signal peptide linked to autosomal-dominant diabetes. Diabetes **61**, 828–837 (2012).
11. Guo H, Y. Xiong, P. Witkowski, J. Cui, L. J. Wang, J. Sun, R. Lara-Lemus, L. Haataja, K. Hutchison, S.O. Shan, P. Arvan, M. LiuInefficient translocation of preproinsulin contributes to pancreatic β cell failure and late-onset diabetes, J Biol Chem **289**, 16290–16302 (2014)
12. Liu, M., Wright, J., Guo, H., Xiong, Y. & Arvan, P. Proinsulin entry and transit through the endoplasmic reticulum in pancreatic beta cells. Vitam Horm **95**, 35–62 (2014).
13. Støy J, J. Olsen, S.Y. Park, S. Gregersen, C.U. Hjørringgaard, G.I. Bell In vivo measurement and biological characterisation of the diabetes-associated mutant insulin p.R46Q (GlnB22-insulin), Diabetologia **60**, 1423–1431 (2017).
14. Nishi M and Nanjyo K Insulin gene mutations and diabetes. *J Diabetes Investig*. **2**, 92–100 (2011). doi: 10.1111/j.2040-1124.2011.00100.x, PMID: 24843467

15. Stefani C Eames, Mary D Kinkel, Sindhu Rajan, Victoria E Prince, and Louis H Philipson, Transgenic zebrafish model of the C43G human insulin gene mutation, *J Diabetes Investig.* **4**, 157–167. (2013), doi: 10.1111/jdi.12015 PMID: 24843647
16. Qinglin Shi and Lijuan Chen, Cereblon: A Protein Crucial to the Multiple Functions of Immunomodulatory Drugs as well as Cell Metabolism and Disease Generation, *J Immunol Res*. 2017, Article ID 9130608 (2017). PMID: 28894755 PMCID: PMC5574216, doi: 10.1155/2017/9130608
17. Cho J, Hiramoto M, Masaike Y, Sakamoto S, Imai Y, ImaiY, Handa H, Imai T*. UGGT1 retains proinsulin in the endoplasmic reticulum in an arginine dependent manner. Biochem Biophys Res Commun **527**, 668–675 (2020). doi: 10.1016/j.bbrc.2020.04.158
18. Cho J, Horikawa Y, Enya M, Takeda J, Imai Y, Imai Y, Handa H, Imai T*. *L*-Arginine prevents cereblon-mediated ubiquitination of glucokinase and stimulates glucose-6-phosphate production in pancreatic β-cells. Commun Biol **3**; 497 (2020).
19. Liu M, R. Lara-Lemus, S.O. Shan, J. Wright, L. Haataja, F. Barbetti, H. Guo, D. Larkin, P. Arvan. Impaired cleavage of preproinsulin signal peptide linked to autosomal-dominant diabetes. Diabetes **61**, 828–837 (2012)
20. Mehmet Adnan Ozturk, Selim Kurtoglu, Osman Bastug, Levent Korkmaz, Ghaniya Daar, Seyma Memur, Hulya Halis, Tamer Günes, Khalid Hussain, Sian Ellard, Neonatal diabetes in an infant of diabetic mother: same novel INS missense mutation in the mother and her offspring, J Pediatr Endocrinol Metab. **27**, 745–8 (2014).
21. Guo H, Y. Xiong, P. Witkowski, J. Cui, L. J. Wang, J. Sun, R. Lara-Lemus, L. Haataja, K. Hutchison, S.O. Shan, P. Arvan, M. Liu. Inefficient translocation of preproinsulin contributes to pancreatic β cell failure and late-onset diabetes, J Biol Chem **289**, 16290–16302 (2014)
22. Ito T, Ando H, Suzuki T, Ogura T, Hotta K, Imamura Y, Yamaguchi Y, Handa H. Identification of a primary target of thalidomide teratogenicity *Science*. **327**, 1345–50 (2005). doi: 10.1126/science.1177319.
23. Juncheng Wei, Yanzhi Yuan, Lu Chen, Yuanming Xu, Yuehui Zhang, Yajun Wang, Yanjie Yang, Clara Bien Peek, Lauren Diebold, Yi Yang, Beixue Gao, Chaozhi Jin, Johanna Melo-Cardenas, Navdeep S. Chandel, Donna D. Zhang, Hui Pan, Kezhong Zhang, Jian Wang, Fuchu He & Deyu Fang. ER-associated ubiquitin ligase HRD1 programs liver metabolism by targeting multiple metabolic enzymes. *Nat Commun* **9**, Article number 3659 (2018).
24. Neha Shrestha, Tongyu Liu, Yewei Ji, Rachel B. Reinert, Mauricio Torres, Xin Li, Maria Zhang, Chih-Hang Anthony Tang, Chih-Chi Andrew Hu, Chengyang Liu, Ali Naji, Ming Liu, Jiandie D. Lin, Sander Kersten, Peter Arvan, and Ling Qi Sel1L-Hrd1 ER-associated degradation maintains β cell identity via TGF-β signaling J Clin Invest. **130**, 3499–3510. (2020) https://doi.org/10.1172/JCI134874.
25. Tijun Wu, Shuang Zhang, Jialiang Xu, Yaqin Zhang, Tong Sun, Yixue Shao, Jiahui Wang, Wei Tang, Fang Chen and Xiao Han HRD1, an Important Player in Pancreatic β-Cell Failure and Therapeutic Target for Type 2 Diabetic Mice Diabetes **69**, 940–953. 2020

26. Eric S. Fischer, Kerstin Böhm, John R. Lydeard, Haidi Yang, Michael B. Stadler, Simone Cavadini, Jane Nagel, Fabrizio Serluca, Vincent Acker, Gondichatnahalli M. Lingaraju, Ritesh B. Tichkule, Michael Schebesta, William C. Forrester, Markus Schirle, Ulrich Hassiepen, Johannes Ottl, Marc Hild, Rohan E. J. Beckwith, J. Wade Harper, Jeremy L. Jenkins & Nicolas H. Thomä. Structure of the DDB1–CRBN E3 ubiquitin ligase in complex with thalidomide. Nature **512**, 49–53 (2014)
27. Christopher Heim,† Dimanthi Pliatsika,‡ Farnoush Mousavizadeh,‡ Kerstin Bär,† Birte Hernandez Alvarez,† Athanassios Giannis,*‡ and Marcus D. Hartmann*†De-Novo Design of Cereblon (CRBN) Effectors Guided by Natural Hydrolysis Products of Thalidomide Derivatives, *J Med Chem*. **62**, 6615–6629. (2019) doi: 10.1021/acs.jmedchem.9b00454 PMCID: PMC6750895 PMID: 31251063
28. Umeda M, Hiramoto M, Watanabe A, Tsunoda N, Imai T*. Arginine-induced insulin secretion in endoplasmic reticulum. Biochem Biophys Res Commun **466**, 717–722, (2015).
29. Uebi T, Umeda M & Imai T*. Estrogen induces Estrogen Receptor alpha expression and hepatocyte proliferation in the livers of the male mice. Genes to Cells **20**, 217–223, (2015) DOI: 10.1111/gtc.12214
30. Umeda M, Hiramoto M & Imai T*. Partial hepatectomy induces delayed hepatocyte proliferation and normal liver regeneration in ovariectomized mice. *Clin Exp Gastroenterol* **8**, 175-182, (2015) PMCID: PMC4494181
31. Tsugawa Y, Natori M, Handa H, and Imai T*. Estradiol accelerates liver regeneration through estrogen receptor α. Clin Exp Gastroenterol **12**, 331–336, 2019. https://doi.org/10.2147/CEG.S214196
32. Tsugawa Y, M. Hiramoto, T. Imai Estrogen induces estrogen receptor α expression and hepatocyte proliferation in late pregnancy, Biochem Biophys Res Commun **511**, 592–596 (2019)
33. Yang Y, Q.X. Hua, J. Liu, E.H. Shimizu, M.H. Choquette, R.B. Mackin, M.A. Weiss. Solution structure of proinsulin: connecting domain flexibility and prohormone processing, J Biol Chem **285**, 7847–7851 (2010).
34. Robert M. Stolz and Brian H. Northrop, Experimental and Theoretical Studies of Selective Thiol–Ene and Thiol–Yne Click Reactions Involving N–Substituted Maleimides, J Org Chem **78**, 8105–8116 (2013).

Figures

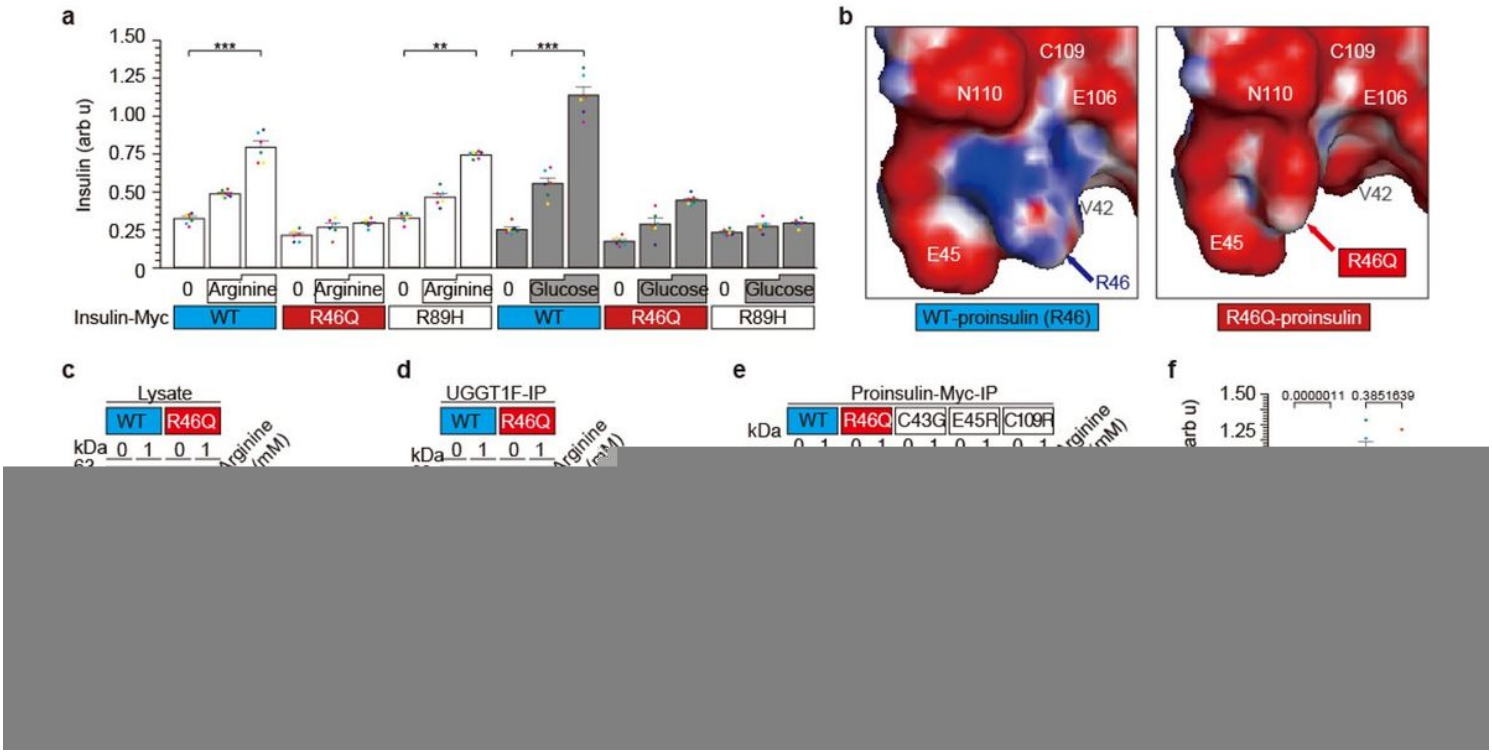

Figure 1

The R46 residue of proinsulin is involved in arginine-induced insulin secretion.

(**a**) The R46 residue of proinsulin is involved in arginine-induced insulin secretion. NIT1 cells transfected with insulin-Myc vectors expressing WT, R46Q, and R89H were preincubated with arginine- or glucose-free F-12K medium for 30 min. Then, the cells were treated with arginine or glucose for 5 min. The culture supernatant was collected, and secreted insulin was analyzed by ELISA. Data are presented as mean ± S.E. n=6 **p < 0.005; ***p < 0.0001.

(**b**) The predicted structure of R46 (WT) and R46Q proinsulin. Protruding R46 residue and surrounding amino acid ring of proinsulin. Basic groups are shown in blue, and acidic groups are shown in red. The original structural data of proinsulin (DOI: 10.2210/pdb3w7y/pdb) were used [33]. The nonprotruding R46Q residue was calculated using PyMOL software. Other directions of the R46 and R46Q structures are shown in Fig. S1a.

(**c**, and **d**) R46Q-mutated proinsulin protein bound to UGGT1 and was retained in the ER with/without arginine. NIT1 cells transfected with WT or R46Q proinsulin were pretreated in arginine-free F-12k for 30 min and stimulated with 1 mM arginine for 5 min. Intracellular proinsulin and UGGT1 were analyzed by WB (**c** and Fig. **S1b**). Proinsulin bound to UGGT1 was assessed by IP of UGGT1 followed by IP-WB (**d** and Fig. **S1c**).

(**e**, and **f**) Three proinsulin variants of the acid ring consisting of V42, C43, E45, E106, C109 and N110 residues of proinsulin were tested for their interaction with UGGT1 along with R46Q proinsulin. Vectors

expressing mutated proinsulin were transfected, and cell lysates were prepared with or without arginine treatment. Proinsulin was immunoprecipitated and blotted for UGGT1 (**c**, **d**, Fig. **S1b**, **S1c** and **S1d**).

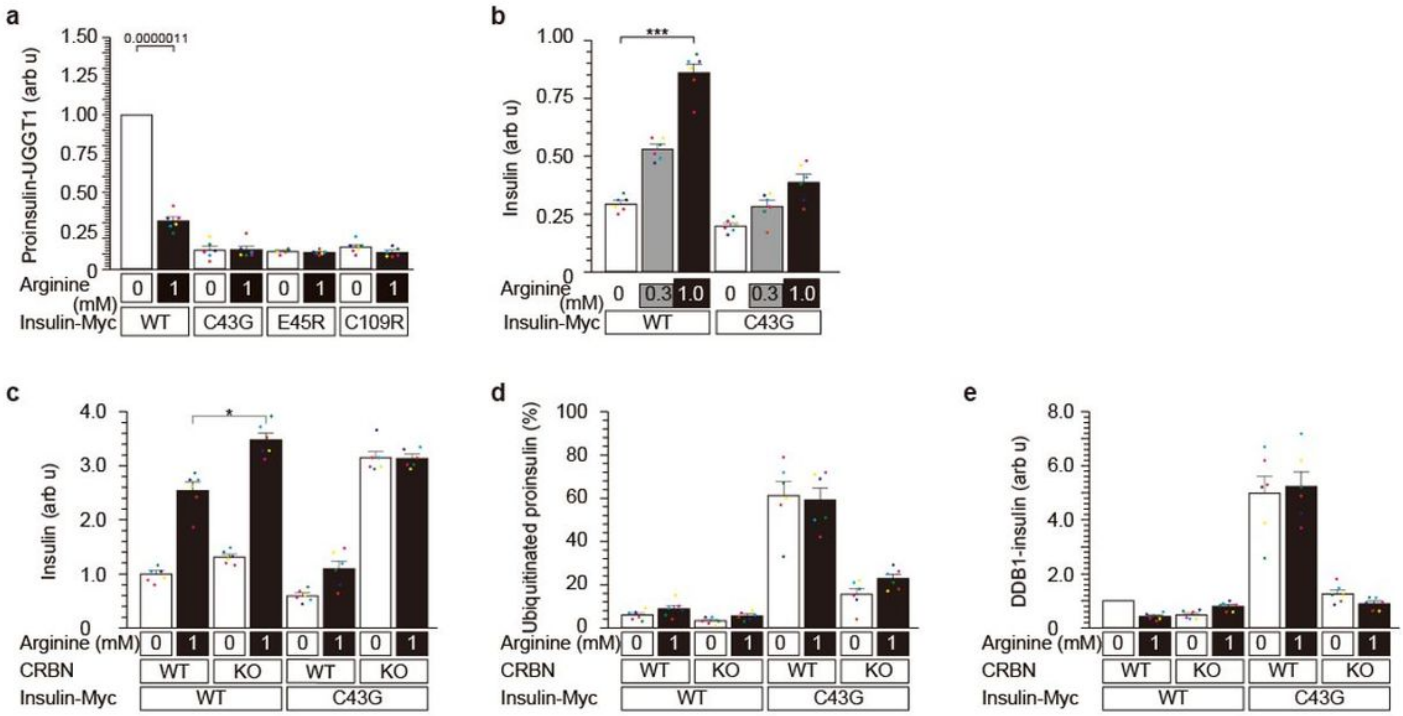

f

People	Insulin	Complex without arginine	Complex with arginine	Ubiquitination	Arginine-induced insulin secretion
Healthy	WT	Insulin+UGGT1	Insulin (free)	Less	Yes
MODY10	R46Q	R46Q+UGGT1	R46Q+UGGT1	Less	N.S.
Neonatal diabetes	C43G C109R	C43G+CRBN+DDB1 C109R+CRBN+DDB1	C43G+CRBN+DDB1 C109R+CRBN+DDB1	Strong	N.S.

Figure 2

Impaired UGGT1-interaction in the C43G-neonatal diabetes variant.

(**a**) Impaired interaction of mutant insulin and UGGT1. WT, C43G, E45R, and C109R insulin were analyzed for their interaction with UGGT1 by immunoprecipitation (Fig **S2a**). All three variants and mutants of acidic amino acid rings failed to bind to UGGT1 in the presence or absence of arginine.

(**b**-**e**) Variant MODY10^{C43G}, a mutation at the acidic amino acid ring, promotes degradation by CRBN and blunts secretion in response to arginine. Arginine-induced insulin^{C43G} secretion was blunted in CRBN^{WT} and CRBN^{KO} cells (**b** and **c**). Ubiquitination of the insulin^{C43G} protein and association with DDB1 were observed only in CRBN^{WT} cells (**d**, **e**, Fig. **S2a** and **S2b**).

(**f**) Summary of the interaction of insulin (R46Q and C43G variants) with UGGT1 and CRBN in the presence and absence of arginine.

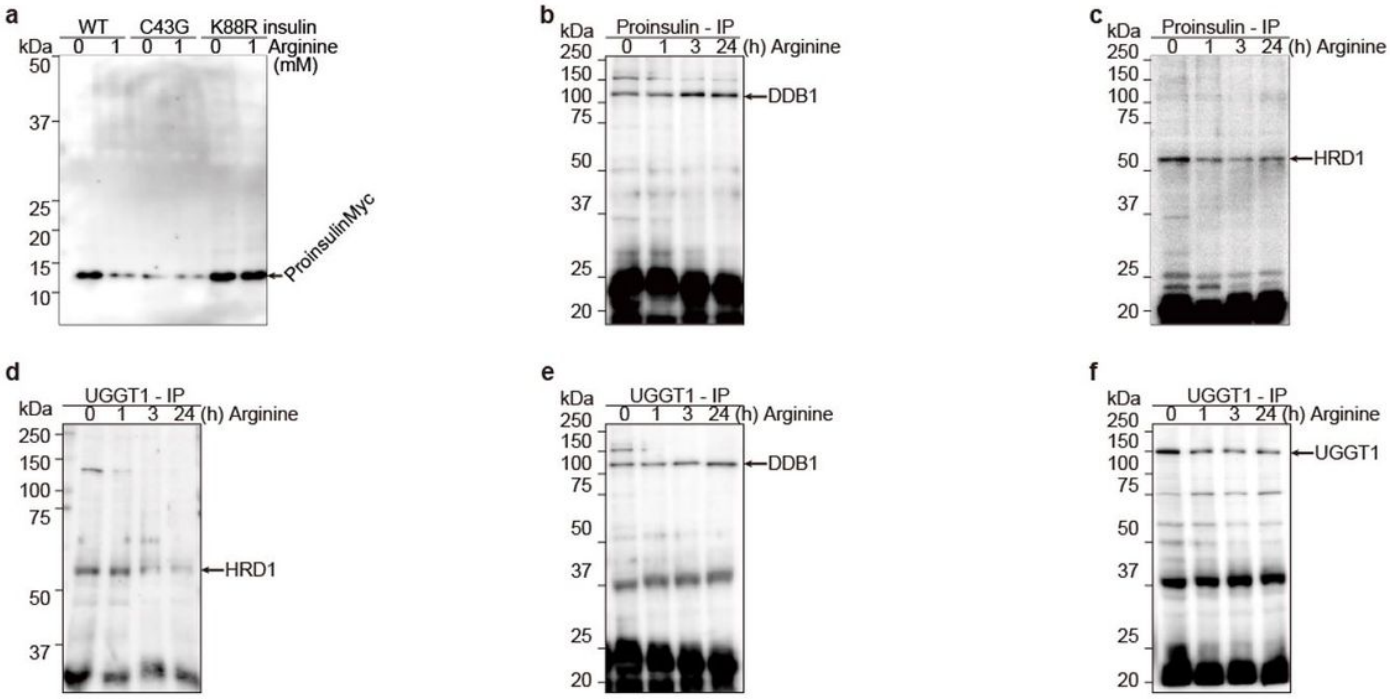

Figure 3

Arginine switches proinsulin associated E3 ubiquitin ligases from HRD1 to CRBN.

(**a**) WT proinsulin was degraded after arginine administration, and C43G proinsulin was degraded with/without arginine, although K88R proinsulin was not degraded with/without arginine. Arginine was depleted for 30 min, and cells were treated with 0 or 1 mM arginine. The cell lysates were visualized with anti-Myc WB.

(**b** - **f**) Both proinsulin and UGGT1 are associated with the E3 ubiquitin ligase DDB1 after arginine administration. Arginine was depleted from the medium for 30 min, and NIT1 cells were treated with 1 mM arginine for the indicated times (0, 1, 3, and 24 h). The cell lysates were IPed with proinsulin (**b** and **c**) or UGGT1 (**d** - **f**), and then these IP-ed lysates were visualized with DDB1 (**b**, and **e**), HRD1 (**c** and **d**), or UGGT1 (**f**, control).

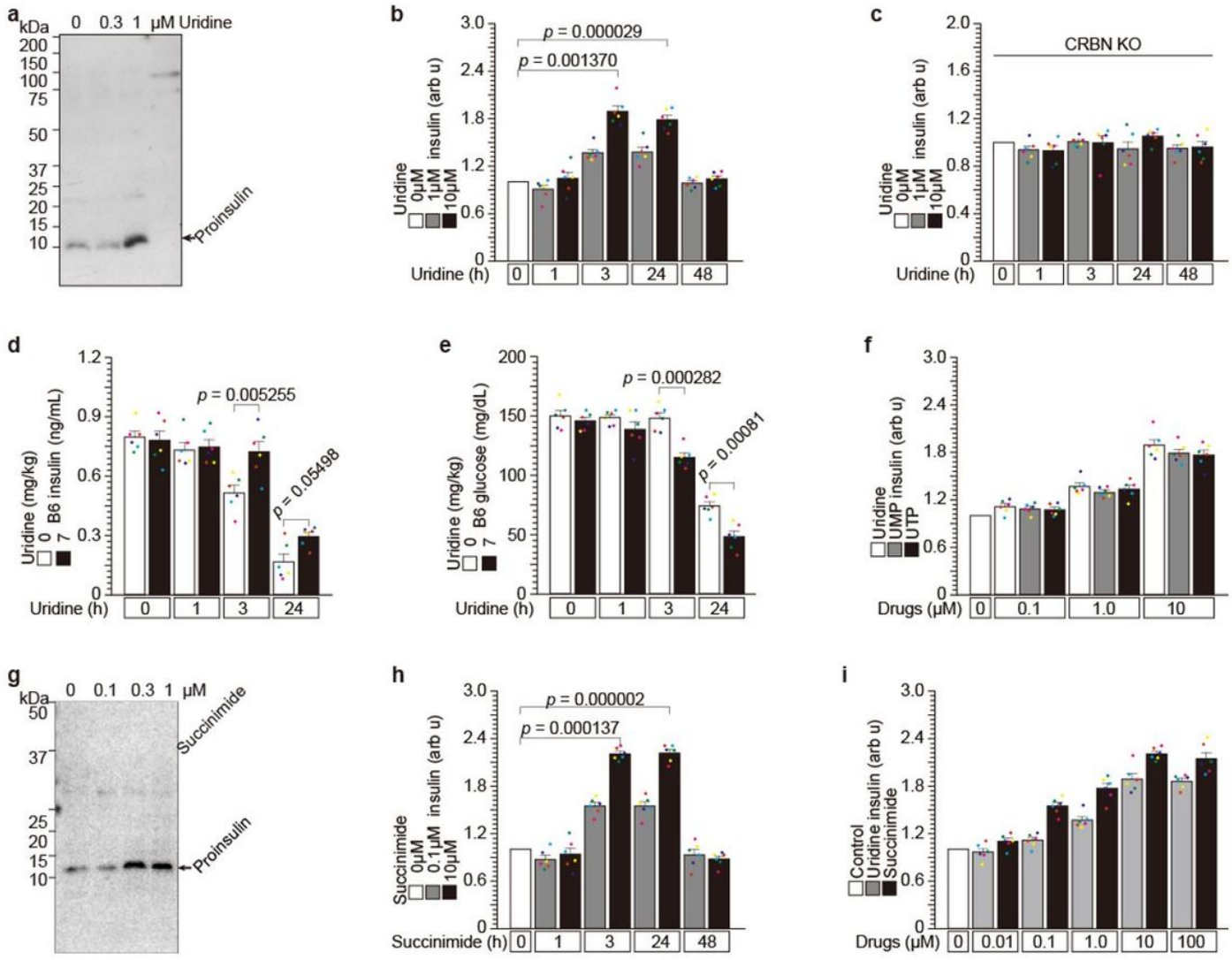

Figure 4

Uridine and succinimide protect proinsulin degradation from CRBN and stimulate insulin secretion from 3 h to 24 h.

(**a**–**e**) Uridine binds to CRBN and protects against proinsulin degradation.

(**a**) Uridine protects against proinsulin degradation in a dose-dependent manner. NIT1 cells were treated with 0, 0.3, or 1 μM uridine for 3 h. Intracellular proinsulin was detected by WB.

(**b** and **c**) Uridine administration to NIT1 cells stimulates insulin secretion from 3 h to 24 h with a CRBN contribution. Uridine was administered to CRBN-WT (**b**) and CRBN-KO (**c**) cells, and insulin secretion was analyzed using ELISA.

(**d** and **e**) Uridine (7 mg/kg) administration to C57/BL6J mice stimulates insulin secretion (**d**) and reduces circulating glucose (**e**) from 3 h to 24 h.

(**f**) Other uridine-containing compounds, UMP and UTP, stimulate insulin secretion from 3 to 24 h.

(**g**-**i**) Succinimide also binds to CRBN and protects against proinsulin degradation.

(**g**) Succinimide protects against proinsulin degradation in a dose-dependent manner. NIT1 cells were treated with 0, 0.1, 0.3, and 1 μM succinimide for 3 h.

(**h** and **i**) Succinimide administration to NIT1 cells stimulated insulin secretion from 3 h to 24 h in a dose-dependent manner.

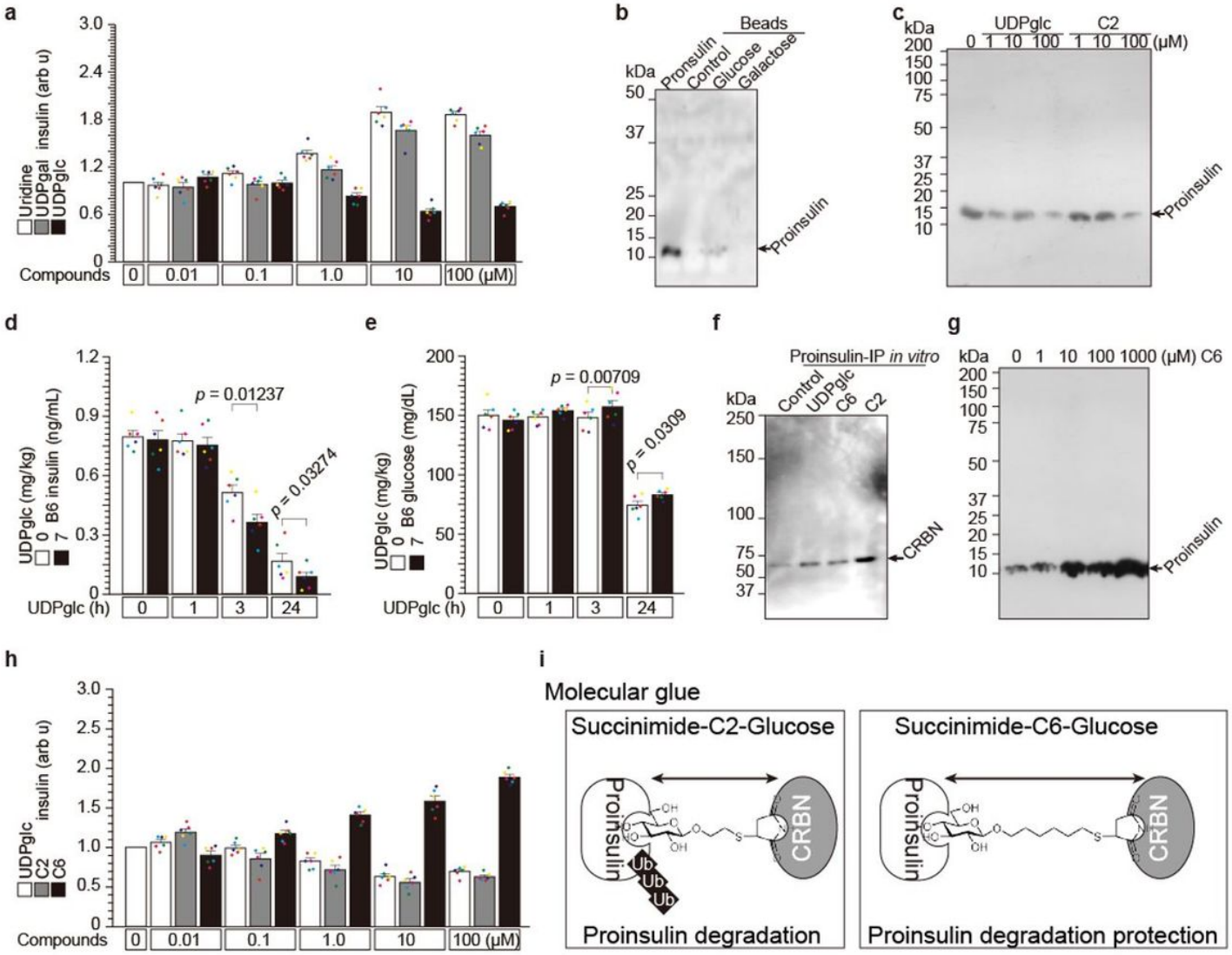

Figure 5

UDP-glucose is an endogenous proinsulin protein degrader through CRBN.

UDP-glucose and succinimide glucose degrade insulin

(**a** and **b**) The proinsulin protein degrader X is UDP glucose. Uridine and UDP galactose administration increased insulin secretion (Fig 4), although UDP glucose decreased insulin secretion in a dose-dependent manner (**a**). Proinsulin binds to glucose but does not bind to galactose (**b**). UDP glucose is a molecular glue between CRBN and proinsulin (**i**)

(**c** and **d**) Administration of the proinsulin protein degrader UDP glucose to C57/BL6J mice decreased circulating insulin (**c**) and increased glucose concentration (**d**).

(**e**-**i**) Succinimide glucose degrades or protects proinsulin.

(**e**) Succinimide-C2-glucose strongly stimulates the proinsulin and CRBN interaction.

(**f**) UDP glucose and succinimide-C2-glucose administration degraded proinsulin protein in NIT1 cells.

(**g**) Succinimide-C6-glucose protects endogenous UDP glucose-dependent proinsulin degradation in a dose-dependent manner.

(**h**) UDP glucose and succinimide-C2-glucose reduced insulin secretion in a dose-dependent manner, although succinimide-C6-glucose induced insulin secretion (like UDP galactose).

(**i**) Possible model of molecular glue with/without proinsulin degradation.

Supplementary Files

This is a list of supplementary files associated with this preprint. Click to download.

- GA.jpg
- 220204Sup.docx